



Full Length Article

Prediction of combustion pressure with deep learning using flame images

Ahmed Maged ^{a,b,*}, Mohamed Nour ^{b,c,*}^a Department of Mechanical Engineering, University of North Texas, Denton, TX, USA^b Mechanical Engineering Department, Benha Faculty of Engineering, Benha University, Benha, Egypt^c School of Mechanical Engineering, Shanghai Jiao Tong University, Dongchuan Road 800, Shanghai, China

ARTICLE INFO

Keywords:

Machine learning
CNN
Deep learning
Cylinder pressure
Combustion
Engine

ABSTRACT

Indicated Mean Effective Pressure

Deep learning methods provide data-driven techniques for handling large amounts of combustion data, thus finding the hidden patterns underlying these data. This study aims to predict combustion pressure from flame images, which provide more comprehensive information about the combustion process than traditional pressure sensors. The flame images were captured from a single-cylinder 4-stroke optical gasoline direct injection (GDI) engine at 1000 rpm, 5.7 bar IMEP, and stoichiometric combustion conditions using a high-speed camera. To achieve this prediction, we employed five different models: EfficientNetB4, ResNet50, Ensemble Adversarial Inception ResNet, convolutional neural network (CNN), and CNN-XGBoost. The training dataset comprised 1350 flame images captured from a single-cylinder optical GDI engine across different combustion stages. To ensure robustness, 150 images were used for validation. The models were subjected to a testing set of 4500 flame images obtained from different cycles, to evaluate how well they could perform on new, unseen data. The results showed that EfficientNetB4 achieved an impressive R^2 of 0.94 and a low RMSE of 0.70 compared to other tested models. Saliency analysis revealed that the model focuses on subtle flame characteristics and areas without intense flames, which suggests that it detects features invisible to the human eye. Additionally, the proposed deep learning approach is applied for the sake of monitoring cycle-to-cycle variations based on in-cylinder flame propagation where it is found that it produces high accuracy compared to those obtained through pressure sensors. Our findings are intended to advance the adoption of machine learning approaches for assisting in engine design and optimization.

1. Introduction

The need for the accurate and efficient prediction of combustion engine performance and emissions has increased with a view to improving engine efficiency, reducing emissions, and eventually optimizing engine designs [1,2]. Between the various parameters governing the operation of a combustion engine, combustion chamber pressure is regarded as one of the most important factors. Combustion chamber pressure data forms primary information for the effective control, diagnosis, and optimization of engine performance. Precise pressure measurements offer valuable insights into combustion stability, efficiency, and knock characteristics. However, obtaining such measurements presents significant challenges, requiring complex experimental setups and considerable effort. Despite these difficulties, the potential for new insights is substantial. Advanced artificial intelligence (AI) tools now enable the analysis of this wealth of data, opening doors to innovation. Recent research has successfully employed machine learning

techniques to enhance engine performance and optimize design [3,4].

The advancement in combustion research and engineering has resulted in an exponential proliferation of data from computation models, experimental investigations, and optical measurements [5]. This massive data reservoir presents immense prospects for the extraction of novel knowledge and insights using methods based on machine learning (ML). Notwithstanding the quick advancements in both ML and combustion investigations, the confluence of these disciplines is still in its nascent stage, presenting a myriad of unexplored research opportunities [6]. The convergence of ML and combustion has the potential to address erstwhile intractable combustion problems and augment the comprehension of intricate combustion mechanisms, thus contributing towards the development of an eco-friendly future [7]. Many of the challenges encountered in the domain of combustion are precisely the kinds of issues that ML seems to be well-suited to solve [8]. Recently, there has been a growing inclination towards exploring the use of image data in a multitude of energy and environmental fields [9]. Researchers have employed various ML algorithms to predict the levels and

* Corresponding authors at: Mechanical Engineering Department, Benha Faculty of Engineering, Benha University, Benha, Egypt.

E-mail addresses: ahmed.maged@unt.edu (A. Maged), mohamed.nour@bhit.bu.edu.eg (M. Nour).

Nomenclature	
AI	Artificial intelligence
ANN	Artificial Neural Network
aTDC	After top dead centre
bTDC	Before top dead centre
CAD	Crank angle degree
CI	Compression ignition
CNN	Convolutional neural network
CO	Carbon monoxide
COV _{P_{max}}	Coefficient of variance
CTC	Cycle-to-cycle variation
DL	Deep learning
GAN	Generative adversarial network
GDI	Gasoline direct injection
GP	Gaussian Process
HC	Hydrocarbons
HCCI	Homogeneous Charge Compression Ignition
ICE	Internal combustion engines
IMEP	Indicated mean effective pressure
LSTM	Long Short-Term Memory
MAPE	Mean Absolute Percentage Error
ML	Machine learning
MLPs	Multilayer perceptron
NG	Natural gas
NO _x	Nitrogen oxides
P _{max}	Peak cylinder pressure
RF	Random forest
RKHS	Reproducing Kernel Hilbert Space
RMSE	Root Mean Square Error
RNN	Recurrent neural network
RVM	Relevance Vector Machine
SI	Spark ignition
SOM	Self-organizing maps
SVM	Support Vector Machine
R ²	Coefficient of Determination
1DCNN	One dimensional convolutional neural network

varyations of physical phenomena, such as materials characteristics [10,11], or toxicity levels of compounds [12], from image data. Furthermore, the application of advanced ML techniques for predicting and deciphering extremely unpredictable in-cylinder processes has garnered substantial attention among combustion experts globally owing to its remarkable analytical and prediction capacities [13]. By capturing images of the combustion process inside the engine and utilizing image processing algorithms to extract pertinent features, it may be feasible to predict diverse parameters and offer valuable insights into the combustion process that are not obtainable through measurement sensors alone.

Lately, various scientists have developed ML algorithms that can identify distinct characteristics of combustion and spray using data obtained from fundamental flame and spray research. Wan et al. [14] presented a combustion zone detection technique by utilizing convolutional neural networks (CNNs) based on the gradient-free regime identification method, which was used for several turbulent flames with multiple zone distinctive features. Similarly, Hwang et al. [15] explored a simple machine learning algorithm that employs linear regression to predict the 3D topology of the spray for a variety of fuels and ambient variables, thereby forecasting complex flash-boiling spray characteristics within spark ignition (SI) engines.

In the domain of combustion engine research, the utilization of ML techniques has the capability of significantly enhancing performance and decreasing pollutants of internal combustion engines (ICE). Owoyele et al. [16] proposed a novel design optimization approach, known as ActivO, which involves the use of an ensemble of ML algorithms that combines weak and strong learner surrogates. They reported that ActivO significantly reduces the time to convergence and number of computational resources needed by 80 %, and this results in a 1.9 % reduction in energy use. Ghazaly et al. [17] developed a unique unsupervised vibration-based identification method to pinpoint the misfire's position in SI engines using Khonen self-organizing maps (SOM). They sought to compare the top qualitative 1D, 2D, and 2D vibration signals to identify the misfire position via an independent neural network. Sahoo et al. [18] employed three different ML methods (Regression Model, Support Vector Machine (SVM), and Artificial Neural Network (ANN)) to predict engine performance, combustion, and emission characteristics. They reported that all performance and emissions parameters were well predicted by a regression algorithm of the third order, while the peak pressure was well indicated by the ANN algorithm.

Fu et al. [19] employed ANN to predict the SI engine efficiency and emissions. They reported that the well-trained ANN algorithm exhibited

excellent performance in forecasting engine efficiency, HC, CO, and NO_x emissions, with a root mean squared error performance metric close to zero when compared to the experimentally measured data. Similarly, Mariaani et al. [20] predicted the in-cylinder pressure of a single-cylinder SI engine employing enhanced extreme ML algorithms. They reported that the IMEP showed an acceptable level of agreement with the experimental findings. Additionally, Liu et al. [21] utilized ANN to predict the exhaust temperature of a HD SI engine running on natural gas (NG). Compared to the physical algorithm, the ML algorithm precisely predicted the exhaust temperature.

In the field of ICE research, ANN is the most used supervised learning algorithm for predicting engine performance and emissions, as reported by Aliramezani et al. [22]. They reported that ANN has some limitations, such as the inability to deal with image data, and the possibility of overfitting for high dimensional data, have not been sufficiently investigated in the field of ICE. They recommend comparing various ML techniques across different applications to more accurately model complex combustion processes (e.g., Relevance Vector Machine (RVM), SVM, Gaussian Process (GP), Artificial Neural Networks (ANN), and Reproducing Kernel Hilbert Space (RKHS)).

Hanuschkin et al. [23] investigated cyclic variations in SI engines by analyzing the early flame kernels using ML techniques. They reported that all the ML techniques they tested—logistic regression, decision tree, and multi-layer perceptron—were capable of forecasting high-energy cycles using only a partial understanding of the flame topology at a particular moment in time during the flame spreading. In another study, Hanuschkin et al. [24] investigated the in-cylinder flow field of a gasoline direct injection (GDI) engine using machine learning methods such as ANN and boosted decision trees (AdaBoost and Gradient Boost).

Hence we can see that traditional ML methods have been widely utilized in the combustion engine field as well as for detecting its cyclic variations with favorable outcomes [25,26], as reported in the review of traditional ML and their application in combustion engines. Meanwhile, Zhao and Hung [13] reported that for high-dimensional feature extraction, such as image-based data, it is challenging to preprocessing the in-cylinder observations using physics. Images-based NNs (such as convolutional neural network (CNN)) have shown to be successful at super-resolving and diminishing engines' data images, that may aid with identifying and exposing spatial and temporal properties. Therefore, deep learning (DL) algorithms like CNNs are advised for complicated thermofluidic applications.

DL has recently been one of the most popular ML methods for forecasting and predicting in-cylinder phenomenon, with impressive results.

DL uses multi-layer representations to wring out hierarchy characteristics from complicated data feeds. Common DL models, such as recurrent neural networks (RNNs), CNNs, and generative adversarial network (GANs) are developed based on NNs architectures [5]. Its exceptional nonlinear regression capacity makes it a suitable method for challenging engine thermofluidic processes predictions [7]. CNNs and RNNs require a substantial amount of data to train. However, CNN has had substantial achievements in pattern and image identification [27].

There are several newer network architectures that offer high flexibility in extracting hidden spatial and/or temporal features from data. However, limited research has been devoted to DL approaches in this regard, which aligns with the findings of Zhao and Hung [13]. Nonetheless, recent studies have shown promising results in utilizing DL for internal combustion engine applications. Ofner et al. [28] presented a DL approach for detecting knock occurrences in ICEs utilizing 1D CNN. The algorithm achieved an accuracy of over 92 % when identifying knocking and non-knocking cycles. Yasar et al. [29] used DNN for predicting engine characteristics such as cylinder pressure in Homogeneous Charge Compression Ignition (HCCI) engines. They compared DNN and ANN methods and found that DNN provided the highest accuracy, with a maximum accuracy of 99.84 % for predicting cylinder pressure.

Gangopadhyay et al. [30] proposed a DL strategy to identify blow-outs in combustion engines. The proposed method outperformed other baseline models for detecting transitions to LBO and is recommended for use in ICEs for real-time performance monitoring due to its high accuracy and computational speed. Lee et al. [31] developed a NO_x prediction model using deep neural networks. This model can predict emission and performance accurately based solely on the engine's operating conditions, without ECU data. Shin et al. [32] utilized the Long Short-Term Memory (LSTM) algorithm to predict exhaust gas emissions with only a few engine data inputs, such as intake and exhaust temperatures and/or injection timings. Unlike conventional techniques, DL showed high accuracy without requiring a lot of vehicle specifications and data. The study successfully predicted nitrogen oxide emissions in a diesel engine and demonstrated that DL may function as a virtual emission analyzer.

Yao et al. [33] utilized a deep ANN with four hidden layers to train DNS of turbulent combustion. According to the authors, choosing training sets wisely can minimize the size of the necessary test dataset by about 50 % without sacrificing the model's accuracy. This approach is highly promising for reducing the computational cost of turbulent spray combustion simulations, which are computationally expensive due to the complexity of the underlying physics and the high dimensionality of the governing equations. The results obtained by Yao et al. [33] indicate that deep ANN-based approaches hold great potential for more efficient and accurate turbulent spray combustion simulations in the future.

For engine performance and combustion features prediction utilizing DL methods, Shin et al. [34] applied DNN in conjunction with chemiluminescence signals from the CH*, OH*, and C₂* radicals to estimate the equivalence ratio of turbulent diffusion flames. Godwin et al. [35] employed ANN and Ensemble LS Boost techniques to predict combustion, performance, and emission parameters of a gasoline engine operating in dual-fueling configuration with ethanol. Huang et al. [1] developed backpropagation neural network models to forecast incylinder pressure, ignition lag, IMEP, combustion timing, and exhaust emissions of NO_x, CO, and UHC for a heavy-duty diesel converted to natural gas SI engine. Ricci et al. [36] combined LSTM+1DCNN models to predict in-cylinder pressure profiles in a three-cylinder SI engine under various operating conditions, aiming to explore the application of advanced machine learning techniques as a substitute for physical sensors. Liu et al. [2] conducted a machine-learning-driven analyses of ammonia combustion performance in a spark-assisted CI engine. In a separate study, Liu et al. [3] random forest (RF) and ANN models for forecasting performance, combustion timing, and exhaust emissions of a diesel engine modified to NG SI engine. Additionally, Liu et al. [4] utilized SVM model to estimate the dynamic performance, including engine

power and torque, of a heavy-duty natural gas SI engine.

The previously discussed research highlighted recent trends in employing machine learning models broadly, and deep learning models specifically, to predict and explain engine performance [21]. The excellent learning and predictive capabilities of ML models and DL models in achieving high-quality engine data predictions is quite promising. A considerable share of existing studies on applying ML and deep learning models in combustion engines has focused on non-image training data. Nevertheless, for high-dimensional features, such as image-based data, it becomes difficult to pre-process in-cylinder data through physics-based methods. Deep learning models are more advisable for complex tasks involving in-cylinder fluid dynamics or flame propagation, as noted by Zhao and Hung [13]. The DL excellent ability to model non-linear relationships makes it well-suited for complex prediction tasks between in-cylinder flame propagation features and engine performance and physical parameters. However, the physical interpretability of deep learning models remains a challenge, reflecting the limited research attempting to connect image-based in-cylinder data with engine performance parameters. Several studies in the literature have applied machine learning and deep learning techniques to forecast combustion pressure [1,29,36]. However, since these models utilized non-image-based data inputs, this provides a key motivation for the present study, which aims to employ deep learning to predict intricate nonlinear relationships between in-cylinder flame features and engine performance metrics such as in-cylinder pressure. Therefore, this study represents a novel approach to predicting combustion pressure using flame image data, potentially paving the way for future research in this area, which targets prediction of physical values for engine parameters from in-cylinder features based on image data.

Another motivation for this research is the potential to obtain additional information about the combustion process that cannot be captured by pressure sensors alone. Flame image data can potentially capture a wide range of features connected to the combustion processes, like the size and shape of the flame, the temperature distribution within the combustion chamber, and the interaction between fuel and air. This is different from sensor measurements, which capture specific parameters at predetermined points, flame images encompass various characteristics of combustion, such as size, shape, and intensity. This holistic view allows for a more detailed analysis of the combustion process and has the potential to uncover insights that sensor data alone may not reveal. Additionally, we present a potential application for addressing cycle-to-cycle fluctuation in ICEs based on in-cylinder flame images. Precisely predicting pressure accurately and efficiently using non-invasive methods with the available amount of data could have significant implications for improving engine efficiency, reducing emissions, and optimizing engine designs.

Although the primary focus of this study is on predicting pressure, the methodology and techniques developed here can be further extended to include other combustion engine parameters such as in-cylinder temperature, spatial mixture distribution, heat release rate, and pollutant emissions based on flame image data. Moreover, the use of image data provides a unique and complementary perspective that can significantly enhance our understanding and optimization of the combustion process. While we acknowledge that implementing high-speed flame image capture in real, multi-cylinder engines, particularly in commercial settings, presents certain challenges, our research serves as an essential proof of concept, paving the way for further development and application.

2. Models architecture

In the proposed methodology, the model takes an input image and outputs a scalar value, representing the predicted in-cylinder combustion pressure. Different models were explored for this task, including ResNet50, EfficientNet, Ensemble Adversarial Inception Resnet, and a custom-built CNN model.

While more models were tested, their performance did not meet expectations. Therefore, only the models with possible utilization were discussed. EfficientNetB4 was selected for its scaling approach, balancing network depth, width, and resolution, which is crucial for processing high-resolution flame images efficiently with fewer parameters. ResNet50 was included due to its proven performance in various image tasks, with skip connections that allow for deeper training and better capture of spatial features in flame images. The Ensemble Adversarial Inception ResNet model was also explored to assess the potential benefits of adversarial training, given the variability in combustion processes. We also developed a custom CNN and CNN-XGBoost models to provide a task-specific baseline. XGBoost was integrated to capture both spatial and non-linear relationships in the data. The custom CNN outperformed the other models in terms of accuracy in predicting pressure values. Interested readers are recommended to refer to the survey by Zhuang et al. [37] for more details on transfer learning and pre-trained models. The explored models were evaluated based on their accuracy and ability to predict pressure values accurately as discussed later in Section 4.

All the explored models are based on the CNN architecture (Fig. 1), which forms the fundamental building block for image processing tasks. The input layer, convolutional layer, activation function layer, pool layer, fully connected layer, and output layer are the six fundamental layers that make up the CNN architecture. Convolutional and pooling layers work together to extract features, and the fully connected layer handles classification. Convolutional kernels or filters serve as representations for the weights and biases of a convolutional layer.

The convolution operation between various input feature maps with convolutional kernels produces an output feature map. The output feature map x_j^l represented as

$$x_j^l = f \left(\sum_{i=1}^{D_{l-1}} x_i^{l-1} * w_{ij}^l + b_j^l \right) \quad (1)$$

is obtained by convolving the previous layer's feature maps x_i^{l-1} with the corresponding convolutional filter w_{ij}^l , and adding the bias term b_j^l , l is the layer number with D number of feature maps, $i, j = 1, 2, \dots, D$, and f activation function. Common activation functions include the Sigmoid function $f(x) = 1/(1 + e^{-x})$ and Rectified Linear Units (ReLU) function $f(x) = \max(0, x)$.

The pooling layer reduces the dimension of the feature maps through downsampling. The output X_j^l of the pooling layer is obtained by applying the pooling function down to the previous layer's feature map x_j^l . Max pooling, where the highest value found inside a subsampling zone is chosen as a new feature, is a common method. The output of the pooling layer is then flattened into a single vector, and weights are applied in the fully connected layer to predict the correct label.

The output of the last convolutional and pooling layers is flattened and fed into one or more fully connected layers, also known as dense layers. These layers are responsible for learning complex relationships between the extracted features and the target variable, enabling the network to make predictions based on the input image.

During the training phase, the goal is to estimate the parameters (w_{ij}^l and b_j^l) that minimize the cost function. The algorithm iteratively adjusts the weights and biases to optimize the model's performance through Adaptive Moment Estimation (Adam).

ResNet50 is a widely used CNN for image classification. It consists of 50 layers and uses skip connections that enable information to flow directly from early layers to later layers, bypassing intermediate layers. This allows the network to learn residual mapping that can be added to the identity mapping, which helps to maintain the gradient signal and enhance the overall functionality of the network. The algorithm is pre-trained on the ImageNet dataset, which is a large-scale dataset consisting of 1.2 million images and 1000 classes. The ResNet50 model was fine-tuned for our task. A schematic of Resnet architecture is illustrated in Fig. 2. More detail on Resnet is available in the work by Kaiming et al. [38].

EfficientNet is a popular convolutional neural network architecture that has achieved state-of-the-art performance on a variety of computer vision tasks, and adopted in different application and studies [39]. EfficientNet differs from other models in that it scales the depth, width, and resolution of the network in a balanced way, allowing it to achieve high accuracy with fewer parameters. To adapt EfficientNet for our regression task, a regression head was added to the final layer. Specifically, the EfficientNetB4 variant was utilized, which has demonstrated strong performance on image classification tasks. The EfficientNetB4 model consists of 15 stages, with the first stage being a stem convolutional layer that extracts features from the input image. The output of the stem layer is passed through a series of blocks, with each block consisting of a set of convolutional layers, followed by batch normalization and activation functions. A schematic of the EfficientNet structure is shown in Fig. 3, although interested readers are encouraged to refer to the literature for more details on the layer sizes and reasoning behind them [40].

Ensemble Adversarial Inception Resnet is a combination of multiple Inception models, each trained on adversarial examples. Adversarial examples are inputs that are specifically crafted to mislead a neural network. By training on these examples, the model becomes more robust to newer inputs. In our study, an ensemble of five Inception models was used, each trained on a combination of the original and adversarial examples. Ensemble Adversarial Inception Resnet is too complicated to be presented by schematic diagrams since it has multiple interactive blocks that might take multiple pages to present, however interested readers can refer to the original work by Kurakin et al. [41].

In addition to exploring pre-trained models, a CNN model was

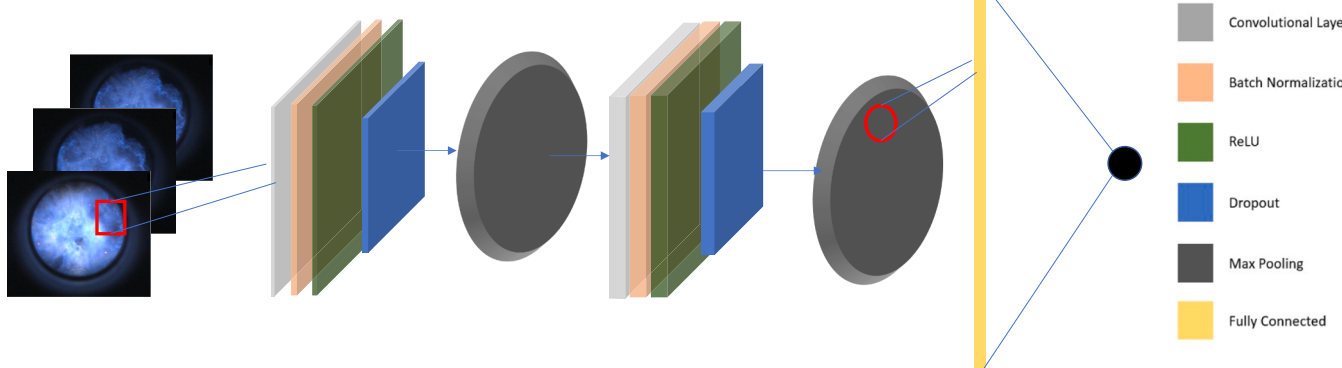


Fig. 1. General architecture of CNNs.

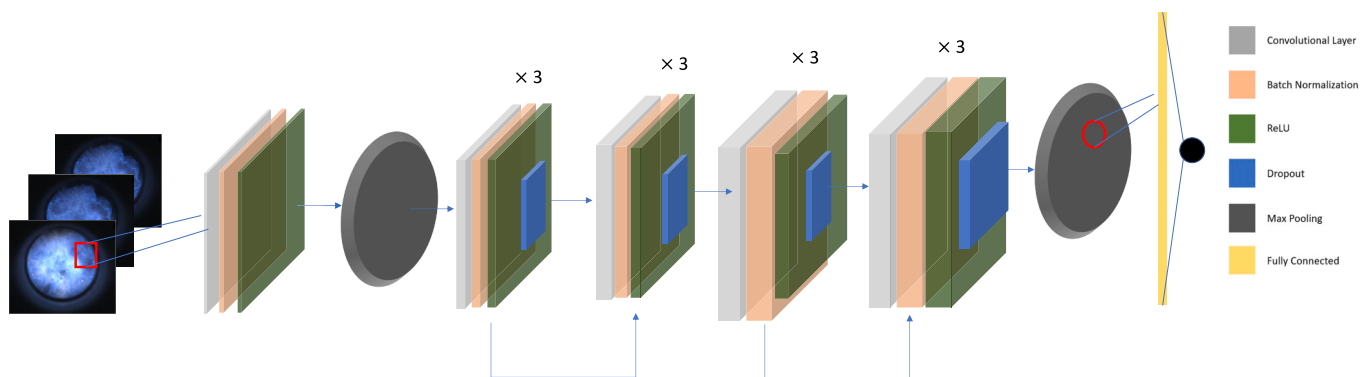


Fig. 2. ResNet simplified architecture of CNNs.

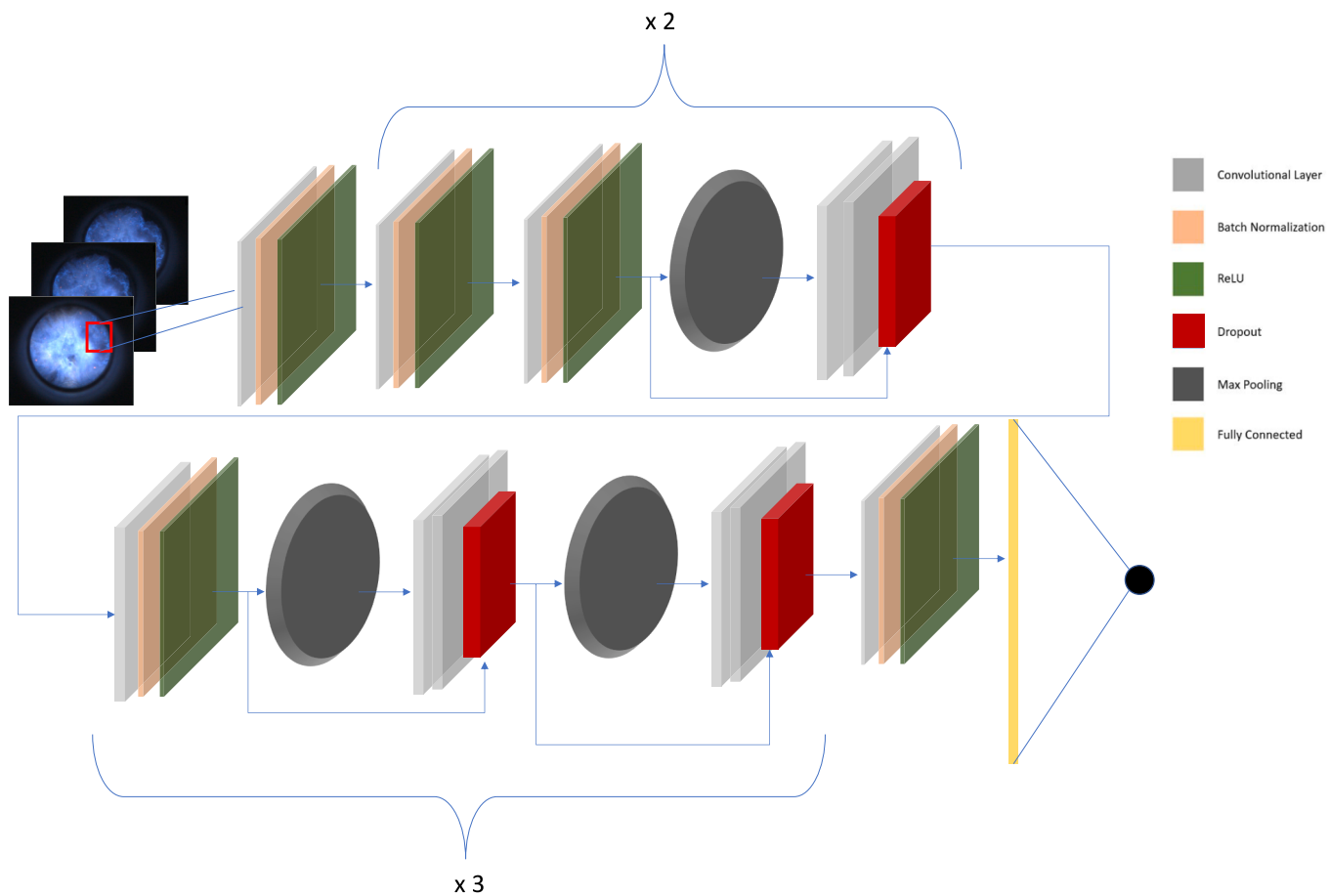


Fig. 3. Schematic presentation of a simplified Efficient architecture.

developed from scratch for this application as presented in Fig. 4(a). And to further ensure that more possibilities were explored, one more stage of a boosting algorithm was added to the extracted features from CNN, which is extreme gradient boosting (XGBoost) as shown in Fig. 4(b). XGBoost is a powerful ML algorithm that belongs to the gradient-boosting family. XGBoost combines several weak-learner prediction models, typically decision trees, into a powerful prediction model. It operates by iteratively adding new models to rectify the faults produced by prior models. Each succeeding model is trained to focus on misclassified or high-error samples, thus gradually improving the overall prediction accuracy [42].

All the pre-trained models were modified by adding a new regression head, which is essentially a linear layer with one output neuron. The

output of this neuron represents the predicted pressure value. To get the input for the regression head, the input image first passes through the models' backbone to extract features. The output of the backbone is subsequently routed via a global average pooling layer to create a fixed-size feature vector, which is then passed through the regression head to generate the final output.

Table 1 presents the used models in this study along with the corresponding number of parameters for each model. The number of parameters varies across the models, ranging from 3,300,000 for the CNN architecture to 54,624,770 for the Ensemble Adversarial Inception Resnet model. These parameter counts reflect the complexity and size of the models, with larger parameter counts often associated with more powerful and sophisticated architectures.

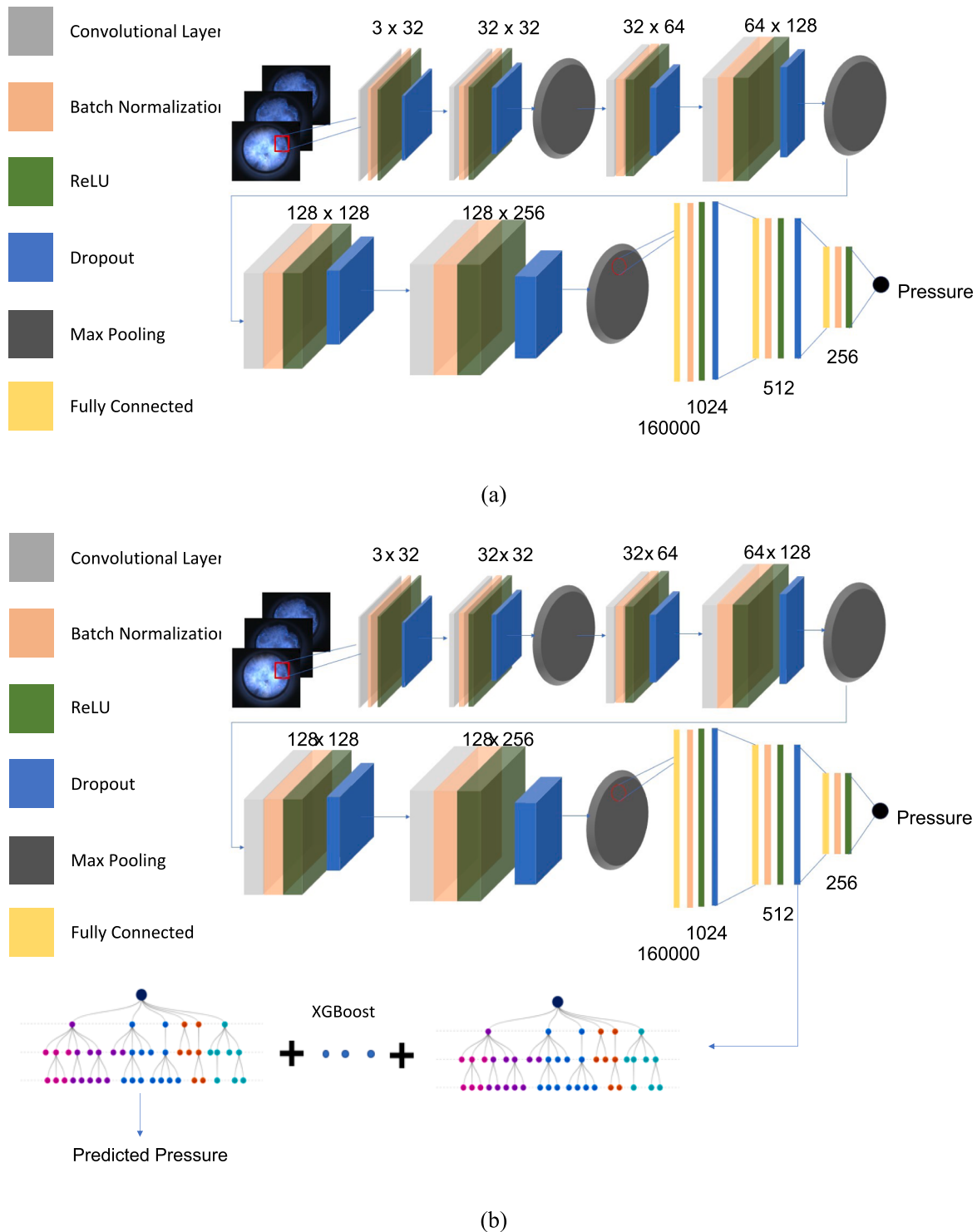


Fig. 4. (a) Developed CNN from scratch for this application (b) CNN with boosting (XGBoost).

Table 1
Trainable parameters of each model.

Model	Number of Parameters (approximately)
EfficientNetB4	17,000,000
ResNet50	23,000,000
Ensemble Adversarial Inception Resnet	54,000,000
CNN	3,300,000
CNN-XGBoost	3,302,000

During training, the model uses mean squared error (MSE) loss to compare its predictions with the true values and updates its weights using backpropagation. The model can then be used to make predictions on new images by passing them through the network and extracting the output from the final layer.

3. Data sampling and Preparation

The data utilized for training and testing in this research was obtained by capturing flame images simultaneously with in-cylinder

本研究中用于训练和测试的数据是通过同时捕获火焰图像和气缸内压力测量得到的，使用的是一台光学研究引擎的测试台。实验配置包括一台单缸 GDI 引擎，配备了光学活塞、火焰传播光学诊断系统和气缸压力测量系统。图 5(a) 展示了实验装置，GDI 引擎和测量系统的技术规格如表 2 所示。实验装置中连接了一个 AC (交流 Alternating Current) 发动机测功机 (AVL)，使得引擎的转速和负载可以在 1000 rpm 和 5.7 bar 负载 (IMEP) 下调节。控制单元 (AVL 型) 用于管理冷却水和润滑油的温度，在整个实验过程中，温度保持在恒定的 60°C。

为了将燃料喷入引擎，采用了一个 6 孔 GDI 博世喷油器 (型号 EA888)，孔径为 0.4 mm。燃料在 10 MPa 的压力下，在 270° bTDC (before Top Dead Center) 时喷入，而点火时机设置为 13° bTDC。该实验装置使得能够获得高质量的火焰图像和压力测量数据，这对于准确训练和测试提出的预测模型至关重要。

本研究中使用的火焰传播诊断系统，如图 5(b) 所示，由一个金属衬里的引擎、一个直径为 62 mm 的光学石英窗口活塞、一个固定在活塞下方的 45° 镜子和一个高速 (CMOS) 相机 (NAC-HX5E) 组成。高速相机与 13° bTDC 的火花点火时机同步，以每 0.5 曲轴角度 (CAD) 捕捉一帧图像，记录火焰通过光学窗口扩展的过程。

pressure measurement, using a test bench of an optical research engine.
The experimental configuration consisted of a single-cylinder GDI engine equipped with an optical piston, a flame-spreading optical diagnosis system, and a cylinder-pressure measurement system. Fig. 5(a) depicts the setup, while technical specifications for the GDI engine and measurement systems are presented in Table 2. An AC dynamometer (AVL) was connected to the engine as part of the experimental setup, allowing for the speed and load of the engine to be adjusted at 1000 rpm and 5.7 bar of load (IMEP). Control units (Type AVL) were utilized to manage the temperatures of the cooling water and lubricating oil, which were maintained at a constant 60 °C throughout the experiment.

To inject the fuel into the engine, a 6-hole GDI Bosch injector (model EA888) with a hole diameter of 0.4 mm was employed. The fuel was injected at a pressure of 10 MPa at 270 bTDC, while the ignition timing was set at 13 bTDC. The experimental setup allowed for the acquisition of high-quality flame images and pressure measurements, which are essential for training and testing the proposed prediction model accurately.

The flame-spreading diagnosis system utilized in this study, as shown in Fig. 5(b), consisted of a metal-lined engine, a piston with a 62 mm-diameter optical quartz window, a 45° mirror fixed beneath the piston, and a high-speed (CMOS) camera (NAC-HX5E). The high-speed camera was synchronized with spark timing at 13 °bTDC and recorded at a rate of one frame per 0.5 crank angle degree (CAD) to capture the flame expanding through the optical window.

To measure the pressure, a system comprising a combustion analyzer, pressure sensor, and amplifier type 2893A, 6125A, and 5064 from Kistler was used. This system recorded the in-cylinder fluctuations of 100 cascading pressure cycles at a resolution of 0.1 CAD. The sampling of pressure data and flame imaging were synchronized for the 100 cascading cycles, ensuring that for each captured set of flame images for any cycle, there was a corresponding measured pressure data for the same cycle. This approach ensured that the flame images and pressure measurements were accurately synchronized and could be used together to train and test the proposed prediction model. The high-speed camera and pressure measurement system used in this study provided high-resolution data that can be utilized to improve the understanding of

Table 2
Specifications of system components.

Item	Parameter	Specs
Engine	GDI engine (one cylinder and 4S) based on 2000 cm ³ GM engine	
	Stroke × Bore	94.6 mm × 86 mm
	Displacement	549.5 cm ³
	CR	11:1
	Fuel injection parameters (pressure, timing, dwell)	10 MPa, 270 °bTDC, 2.45 ms
	Ignition parameters (timing)	13 °bTDC
	T _{cooling water} / T _{hub oil}	60 °C
	Speed	1000 rpm
	λ	1
	Swirl ratio and tumble ratio	0.55 and 0.5
Cylinder pressure measurement	Kibox (2893A), Kistler (6125A), Kistler (5064)	Pressure reading each
Flame high-speed images	– Camera (NAC HX-5E RGB) – lens (Zeiss 50 mm f/1.4)	0.1 CAD – One flame image each 0.5 CAD – Recording frequency of 12000 Hz

the combustion process and optimize engine performance.

Fig. 6 displays the difference in in-cylinder pressure variation between two different cycles, along with flame images illustrating the distinct flame propagation features of each cycle, as shown in Fig. 6(a). By training a deep learning model, the pressure values can be predicted based on the provided flame images with different sets of features. The pressure data sampling process and flame image capturing were synchronized, as illustrated in Fig. 6(b), where the average in-cylinder pressure was sampled every 0.1 crank angle degree, while the flame image was captured every 0.5 crank angle degree. The sampling points of pressure and capturing points of flame were detailed in Fig. 6(b) for the pressure data from 10 to 15 aTDC, outlined with a box in Fig. 6(a). It is evident from the F and P frequency in Fig. 6(b) that every 5 sampled pressure points correspond to one captured flame image.

After the flame sampling process, the obtained raw data of flame images underwent post-processing using a developed code to produce clearer images. The post-processing process began with cropping the

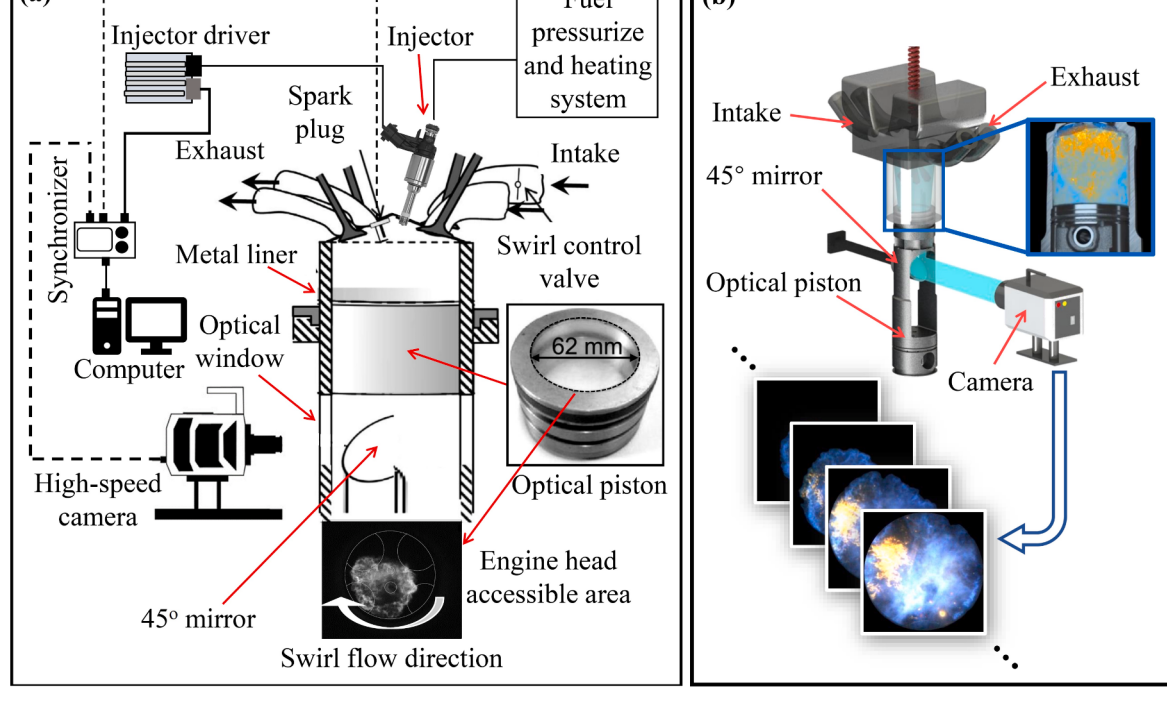


Fig. 5. Layout for optical engine setup (a) Over all engine setup (b) flame visualization.

为了测量压力，使用了由 Kistler 提供的燃烧分析仪、压力传感器和放大器 (型号 2893A、6125A 和 5064)。该系统记录了 100 个连续压力周期的气缸内压力波动，分辨率为 0.1 CAD(Crank Angle Degree)。压力数据的采样和火焰图像的捕捉是同步进行的，对于每个捕获的火焰图像数据集，都有相应的同周期的压力数据。这种方法确保了火焰图像和压力测量数据的准确同步，从而能够一起用于训练和测试预测模型。本研究中使用的高速相机和压力测量系统提供了高分辨率的数据，可用于提高对燃烧过程的理解并优化引擎性能。

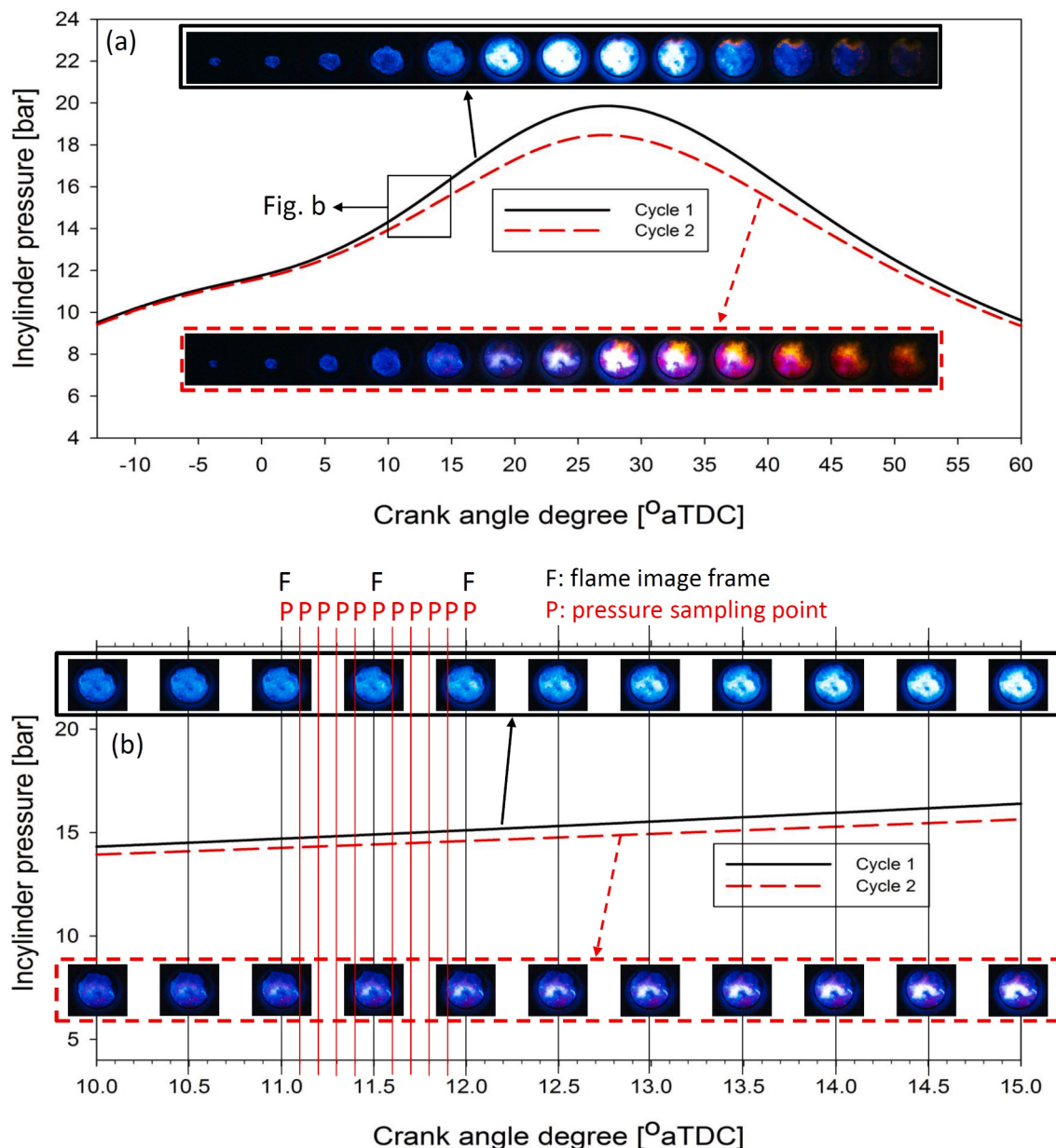


Fig. 6. Data sampling illustration and synchronization between flame image data and pressure data (a) from -13 to 60 aTDC (b) From 10 to 15 aTDC.

raw image to the optical window size, which is the flame visualization area, followed by applying a mask to enable a black background and remove the hollow reflections from the cylinder wall. The image was then binarized, and a median filter was applied to help reduce the flame noise. Finally, after the image matrix point multiplication, the final images were used after noise reduction, as shown in Fig. 7. The post-processing step was essential to produce high-quality flame images that can be used to train and test the proposed prediction model accurately.

4. Models training and performance Evaluation

All models were trained on a dataset of 1350 images (9 cycles) and used 150 images (1 cycle) for validation, allowing for progress monitoring and adjustments during training. After training, the model's accuracy was tested on a large testing set of 4500 images (30 cycles). A total of 40 cycles were used for training, validation, and testing.

In the field of DL, it is worth noting that 1350 samples can be

considered sufficient for similar applications. A research group from General Motors [43] utilized 357 images (213 for training, 72 for validation, and 72 for testing) in their model development, capturing a single frame during each cycle at a specific crank angle. Hanuschkin et al. [23] developed their model using a selection of 615 images from ten experimental runs, each consisting of 350 cycles. They captured a single frame (flame image) in each cycle at a specific crank angle and combustion phase. Another study by Hanuschkin et al. [24] involved capturing frames at intervals of every 4 CAD over numerous cycles for ML model development.

Despite other researchers seemingly using more cycles, it is important to note that our study trained the model using more images and features than the existing literature. Our focus was on capturing flame images at a higher resolution every 0.5 CAD to predict pressure values throughout the entire cycle, rather than specific combustion phases at certain crank angle degrees. Additionally, the selection of cycles for training was strategic, encompassing variations in combustion that the engine might exhibit, including low, medium, and high-pressure cycles.

火焰采样完成后，获得的原始火焰图像数据经过后处理，使用开发的代码进行清晰化处理。后处理过程首先对原始图像进行裁剪，裁剪成光学窗口的大小，这是火焰可视化区域，随后应用遮罩来启用黑色背景并去除气缸壁的空心反射。然后对图像进行二值化，并应用中值滤波器来帮助减少火焰噪声。最后，经过图像矩阵的点乘，去除噪声后的最终图像被用于训练和测试预测模型，确保了高质量的火焰图像能够用于准确的模型训练和测试。

在深度学习领域，值得注意的是，1350个样本对于类似应用来说可以认为是足够的。通用汽车（General Motors）的一组研究人员[43]在他们的模型开发中使用了357张图像（213张用于训练，72张用于验证，72张用于测试），每个循环在特定的曲轴角度下捕获一帧图像。Hanuschkin等人[23]则使用了从十次实验中选取的615张图像进行模型开发，每次实验包括350个循环。他们在每个循环的特定曲轴角度和燃烧阶段捕获一帧图像。Hanuschkin等人[24]的另一项研究涉及在多个循环中以每4个曲轴角度（CAD）的间隔捕获图像用于机器学习模型开发。尽管其他研究者使用了更多的循环数据，但值得注意的是，我们的研究使用了更多的图像和特征进行模型训练，而不仅仅是在特定的燃尽阶段或特定的曲轴角度下捕获图像。我们的重点是每0.5 CAD捕获更高分辨率的火焰图像，以便预测整个循环过程中的压力。此外，训练循环的选择具有战略性，涵盖了发动机可能表现出的不同燃烧情况，包括低压、中压和高压循环。在训练阶段，优先评估了模型预测压力的能力，使用 200×200 大小的图像（相当于4000个输入特征），并确保选择了具有代表性的循环数量，以避免过度的数据拟合。如前所述，我们使用了迁移学习技术，这使我们能够从知识丰富的起点开始训练，从而减少了对更大数据集的需求。此外，还应用了多种数据增强技术，以增强训练集的多样性，从而提升模型的鲁棒性，避免过拟合[44]。这些技术包括图像镜像（水平翻转）、小范围旋转（最多 $\pm 10^\circ$ ）、亮度调整（在 $\pm 10\%$ 的范围内）和随机裁剪并调整大小到原始尺寸。通过在训练过程中引入这些变化，我们增加了数据集的大小，并提高了模型在不同燃烧条件下的泛化能力。这种方法帮助模型变得更加能适应火焰方向、亮度和位置的微小变化，这在现实世界中是常见的。为了模拟实际应用，模型的鲁棒性在30个循环、4500张图像的独立测试集上进行了测试。通过在一个独立的、未见过的测试集上测试模型，我们评估了模型的泛化性能，确定了它在新的、未见过的数据上的表现。这是评估机器学习模型有效性的第一步，因为它确保了算法不会过拟合训练数据集，并能够对未见过的数据集进行泛化。此外，在大型数据集上进行测试有助于更准确地估计模型在实际场景中的性能。最后，这也评估了模型在迁移学习中的表现，即它如何适应全新且不熟悉的条件。值得注意的是，在现实中，如果某些新的条件下的图像数据可用，可以对模型的参数进行微调。

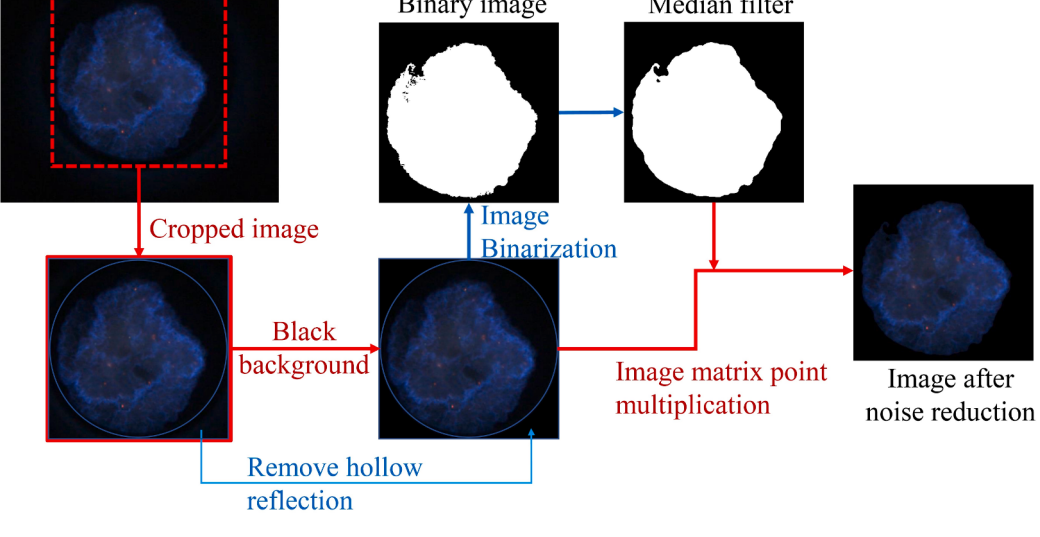


Fig. 7. Flame images postprocessing.

During the training phase, evaluating the model's ability to predict pressure using 200×200 -sized images (equivalent to 4000 input features) over a representative number of cycles was prioritized to avoid excessive computational strain. As earlier discussed, we used transfer learning techniques, which allowed us to initiate the training process from a knowledge-rich starting point, thereby reducing the need for a more extensive data set. Additionally, several data augmentation techniques were applied to synthetically expand the diversity of our training set, thereby enhancing the robustness of the model against overfitting [44]. These included image mirroring (horizontal flipping), small random rotations (up to ± 10 degrees), brightness adjustments (within a $\pm 10\%$ range), and random cropping with resizing to the original dimensions. By introducing these variations during training, we increased the dataset size as well as improved the model's ability to generalize across different combustion conditions. This approach helped the model become more invariant to minor changes in flame orientation, brightness, and positioning, which are typical in real-world scenarios.

To imitate practical application, the model's robustness was tested on a separate set of 30 cycles containing 4500 images. By testing the model on a separate unseen testing set, the generalization performance of the model was evaluated to determine how well it could perform on new, unseen data. This is an important step in evaluating the effectiveness of a ML model, as it ensures that the algorithm is not overfitting to the trained dataset and can be generalized to unseen dataset. Additionally, testing on a large data set can help to show a more accurate estimation of the model's performance in real-world scenarios. Finally, this evaluates how well the model performs at transfer learning, adapting to entirely new and unfamiliar conditions. Note that in realistic situations, one could fine-tune the model's parameters if some image data from the new condition becomes available. The predictive accuracy of the model was evaluated using three key metrics:

- Mean Absolute Percentage Error (MAPE) which calculates the average percentage difference between predicted and actual values.

$$MAPE = \frac{1}{n} \sum_{i=1}^n \left| \frac{y_i - \hat{y}_i}{y_i} \right| \times 100\% \quad (2)$$

- Root Mean Squared Error (RMSE) that represents the difference between predicted and actual values.

$$RMSE = \sqrt{\frac{1}{n} \sum_{i=1}^n (y_i - \hat{y}_i)^2} \quad (3)$$

- Coefficient of Determination (R^2) which determines how well the model fits the data by calculating the proportion of variance in the dependent variable that can be attributed to the independent variable.

$$R^2 = 1 - \frac{\sum_{i=1}^n (y_i - \hat{y}_i)^2}{\sum_{i=1}^n (y_i - \bar{y})^2} \quad (4)$$

where y_i is the actual value of the target variable for the i^{th} data point, \hat{y}_i is the predicted value of the target variable for the i^{th} data point, \bar{y} is the mean value of the target variable across all data points, and n is the total number of data points. Table 3 summarizes the performance of the used models during the training and testing stages.

For the test set, the R^2 values were calculated for each model and obtained insightful results, which were presented using a box plot (Fig. 8). The analysis of R^2 values clearly demonstrates that EfficientNetB4, outperforms all the other models included in the comparison. The box plot shows that the box corresponding to our model exhibits a narrower spread compared to the other models, indicating a higher degree of consistency in performance across the 30 cycles.

Among the other models, ResNet50 shows a relatively narrower box, suggesting a comparable level of consistency in performance. However, it is worth noting that our model consistently achieves higher R^2 scores

Table 3
Performance of the studied networks.

Model	Training			Testing		
	R^2	RMSE	MAPE	R^2	RMSE	MAPE
EfficientNetB4	0.97	0.46	4.79	0.94	0.70	4.79
ResNet50	0.91	0.81	7.05	0.89	0.98	7.05
Ensemble Adversarial Inception	0.83	1.17	8.38	0.80	1.36	8.38
CNN	0.95	0.83	7.55	0.93	1.01	7.55
CNN-XGBoost	0.96	0.76	7.18	0.93	1.07	7.18

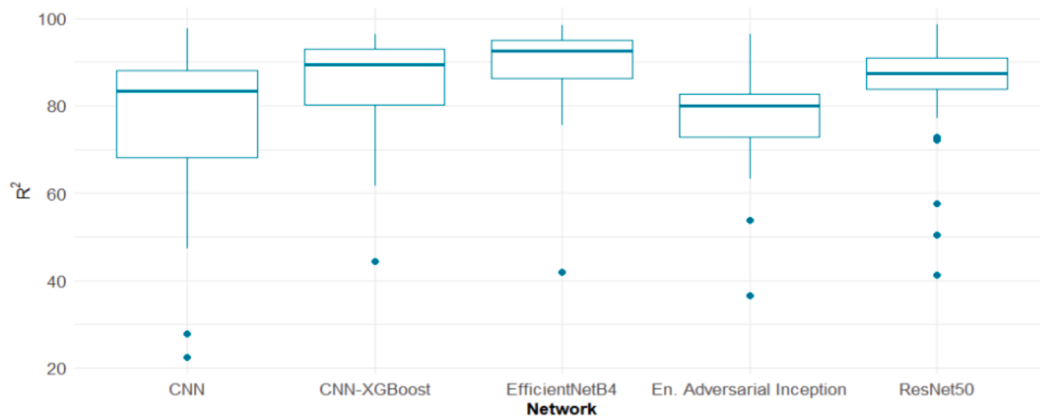
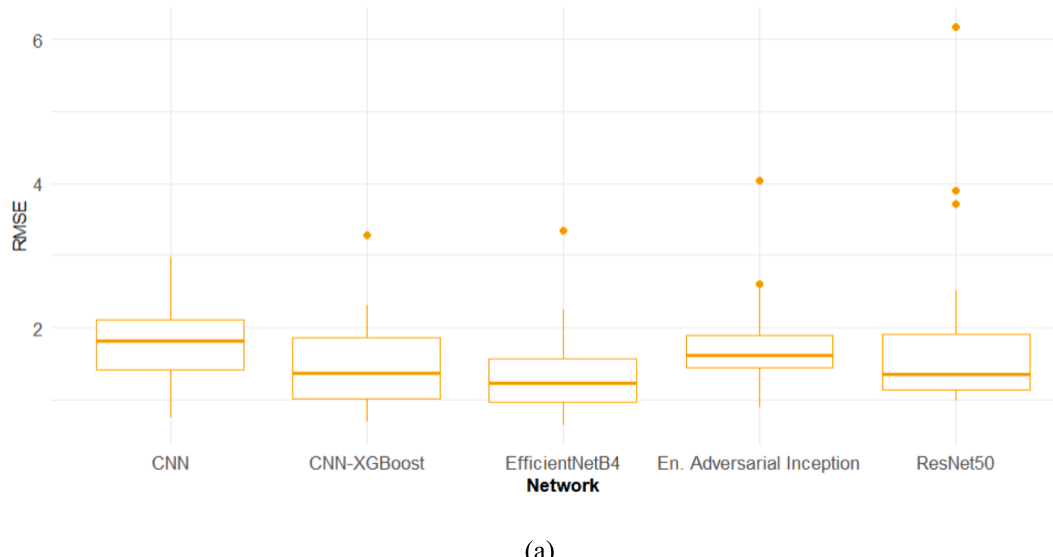


Fig. 8. Box plot of R^2 for each network.

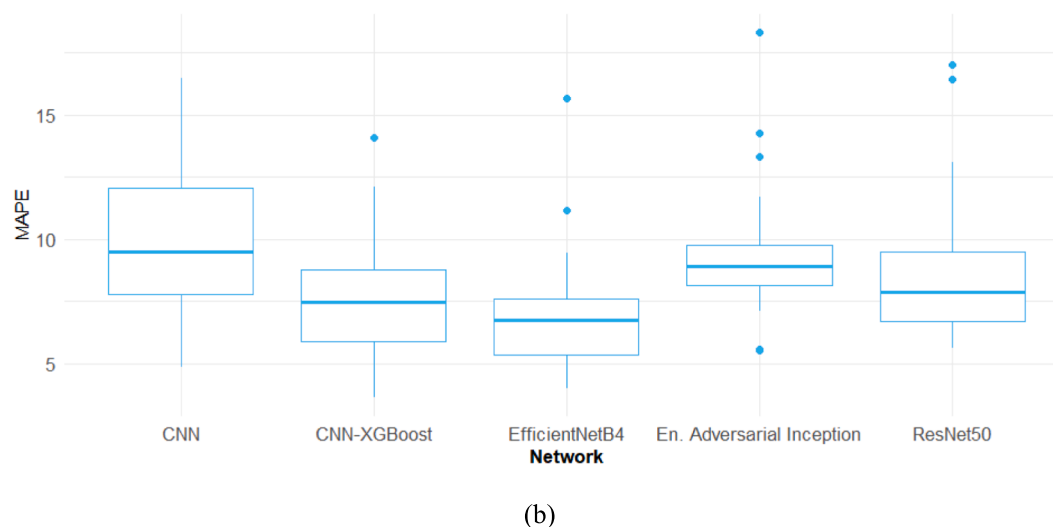
across all cycles, showcasing its superior predictive capability. In contrast, Ensemble Adversarial Inception, CNN, and CNN-XGBoost exhibit wider boxes, indicating greater variability in performance across the cycles. These models demonstrate lower R^2 scores on average compared to both EfficientNetB4 and ResNet50. This variability in

performance can be attributed to the inherent complexity of the models and their sensitivity to different cycle conditions.

Similarly, the RMSE and MAPE values were calculated for each model's predictions. The results are presented also using box plots in Fig. 9 to facilitate a visual comparison. Upon analyzing the box plots, it



(a)



(b)

Fig. 9. Box plot of (a) RMSE (b) MAPE for each network.

is evident that EfficientNetB4, consistently outperforms the other models in terms of both RMSE and MAPE. Furthermore, the box plot also reveals that the boxes for EfficientNetB4 are relatively small, suggesting less variability in prediction errors across the 30 cycles. This consistency in performance is crucial for applications that require accurate and reliable predictions, especially in the presence of cycle-to-cycle variation.

Comparatively, the other models, including ResNet50, exhibit larger medians and wider boxes in both RMSE and MAPE. This indicates higher levels of prediction errors and greater variability in performance across the cycles. These models tend to have less robust performance and may be more affected by cycle-to-cycle variations.

The mean performance of each network was reported across the entire dataset, considering the three performance measures. Fig. 10 illustrates the bar plots showcasing the mean performance of each network for the entire dataset. EfficientNetB4 achieved the highest mean value of R^2 and the smallest RMSE and MAPE compared to the other models. This further supports its efficiency in representing cycle-to-cycle variation and producing accurate predictions for the target variable.

To gain further insights into the performance of EfficientNetB4 in presenting cycle-to-cycle variation, a detailed analysis was conducted by plotting the predicted versus actual values for 20 cycles from the dataset. This analysis allows us to examine the overall agreement between the predicted and actual values and identify any potential anomalies or inconsistencies. Fig. 11 illustrates the scatter plot with a regression line representing the predicted versus actual values for the 20 cycles using EfficientNetB4 model.

Upon visual inspection, the scatter plot demonstrates a generally positive correlation between the predicted and actual values. The regression line, which represents the overall trend, exhibits a good fit to the data points, indicating a reliable estimation of the target variable. It is important to note that in real-life scenarios, certain cycles may exhibit variations or outliers due to various factors such as operational conditions, measurement errors, or unexpected events. In our analysis, it was observed that one cycle (Cycle 7) appeared to deviate from the overall trend. This finding is expected and aligns with the inherent variability encountered in practical applications.

The performance of the proposed models was evaluated for predicting the pressure values for each cycle. The ability of the model to predict cycle-to-cycle variation is also considered. Fig. 12 shows a plot of

average cycle from predicted data and average cycle from measurement data. Upon examination, a high level of agreement was observed between the average predicted and actual values, with minimal deviations. The peak pressure values are the same. However, the peak pressure of predicted cycles was slightly earlier than that of the measured one. This could be due to the flame propagated to reach the wall where the trained models predicted the point of the maximum pressure earlier than the actual measured peak pressure. The prediction of combustion characteristics from flame propagation and images are timely compared to pressure sensor as can be concluded from literature [44].

To assess the model's performance across different measuring angles within complete cycles, the actual and predicted values for 10 complete cycles against the measuring angle were plotted. This analysis enables us to evaluate the model's accuracy and consistency in capturing the variations throughout the entire cycle. Fig. 13 illustrates the plot of the actual and predicted values against the measuring angle for the selected cycles. Upon inspection, a consistent alignment was observed between the actual and predicted values across the measuring angle. This indicates that our EfficientNetB4 model successfully captures the underlying patterns and trends in the data, resulting in reliable predictions throughout the entire cycle. These two plots demonstrate the model's capability to produce accurate and consistent predictions in scenarios with small differences between the mean predictions and actual values and when considering the measuring angle within complete cycles. These findings support the effectiveness of our EfficientNetB4 model in providing reliable predictions for the target variable.

By investigating these specific scenarios, a deeper insight was gained into the model's performance and its ability to handle variations in different aspects of the data. This analysis further reinforces the overall effectiveness and reliability of our EfficientNetB4 model in real-world applications.

5. Cycle-to-Cycle variation assessment using the proposed network

Monitoring the fluctuations in the combustion process from cycle to cycle in engines is important because it can yield useful information about the engine's performance and efficiency. Cycle-to-cycle (CTC) variation, which refers to the differences in combustion that happen from one cycle to the next, can arise due to several factors, such as the

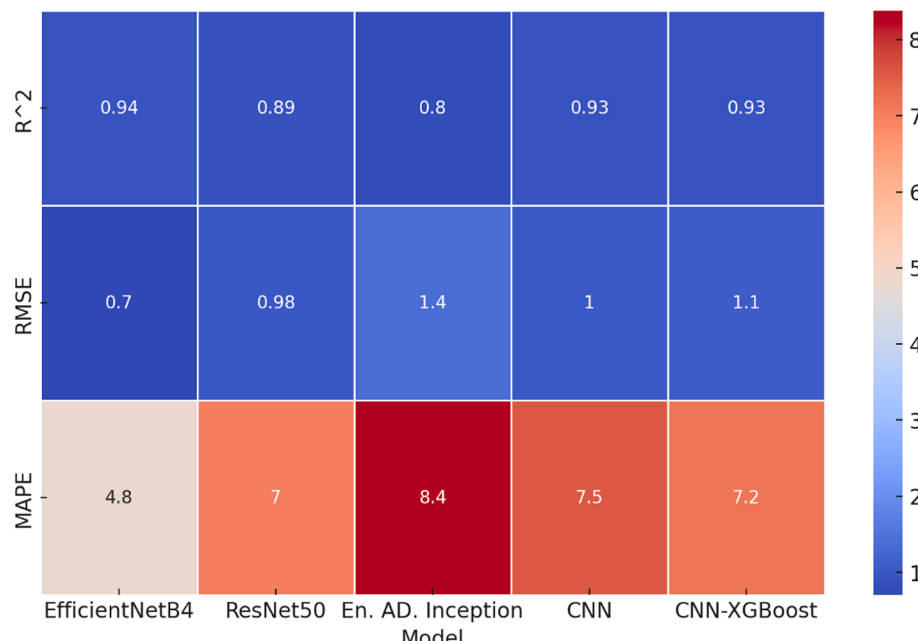


Fig. 10. Heatmap of the Mean of R^2 , RMSE, and MAPE.

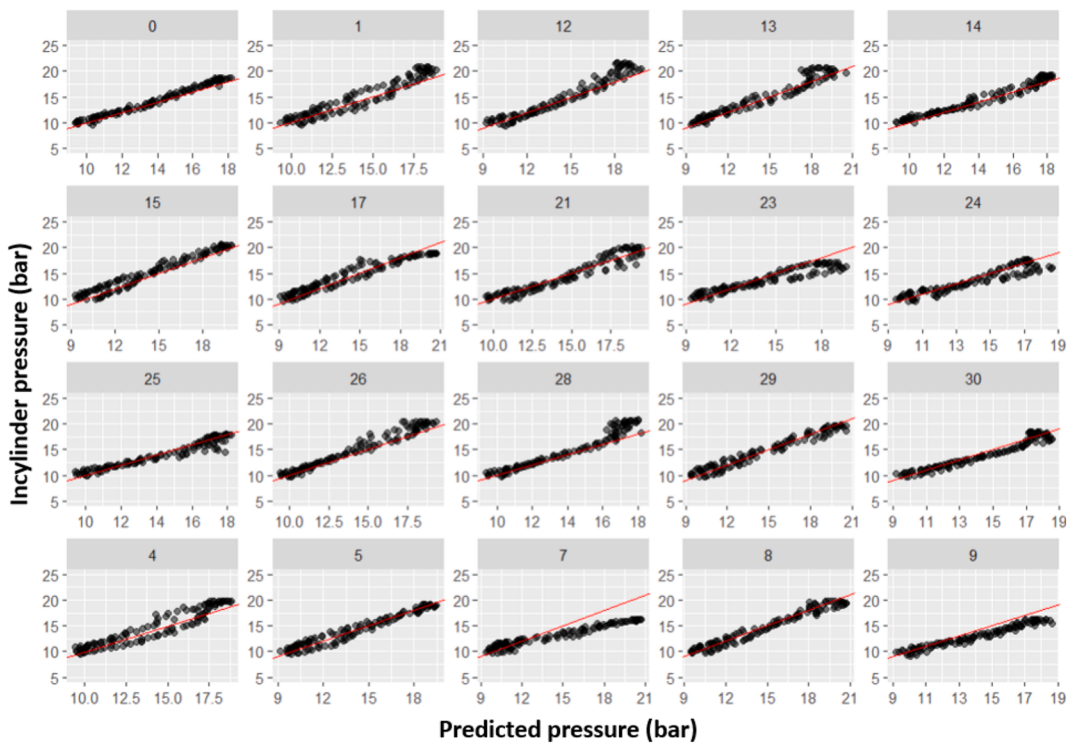


Fig. 11. Predicted vs actual in-cylinder pressure values for 20 cycles.

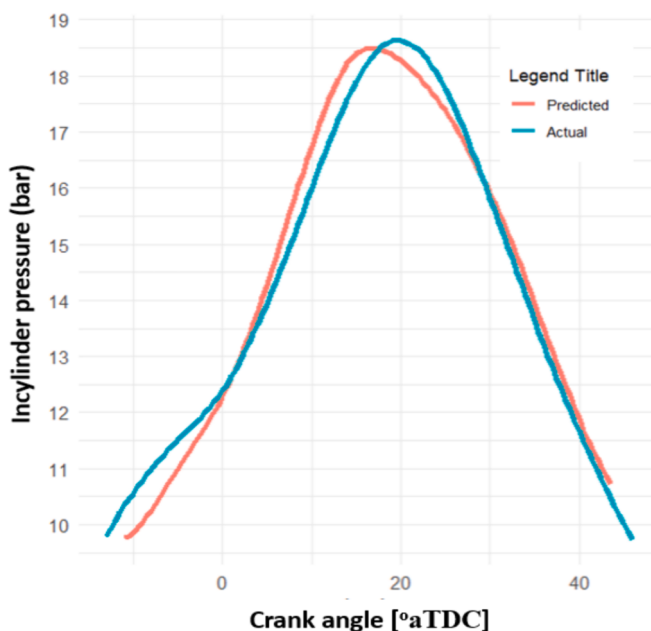


Fig. 12. Comparison of the average pressure cycles from measured and predicted data.

fuel-air ratio, ignition timing, engine load, etc. By measuring CTC variation, trends and patterns in the combustion process can be spotted and used to enhance engine performance and serve as an early indicator of engine operation stability.

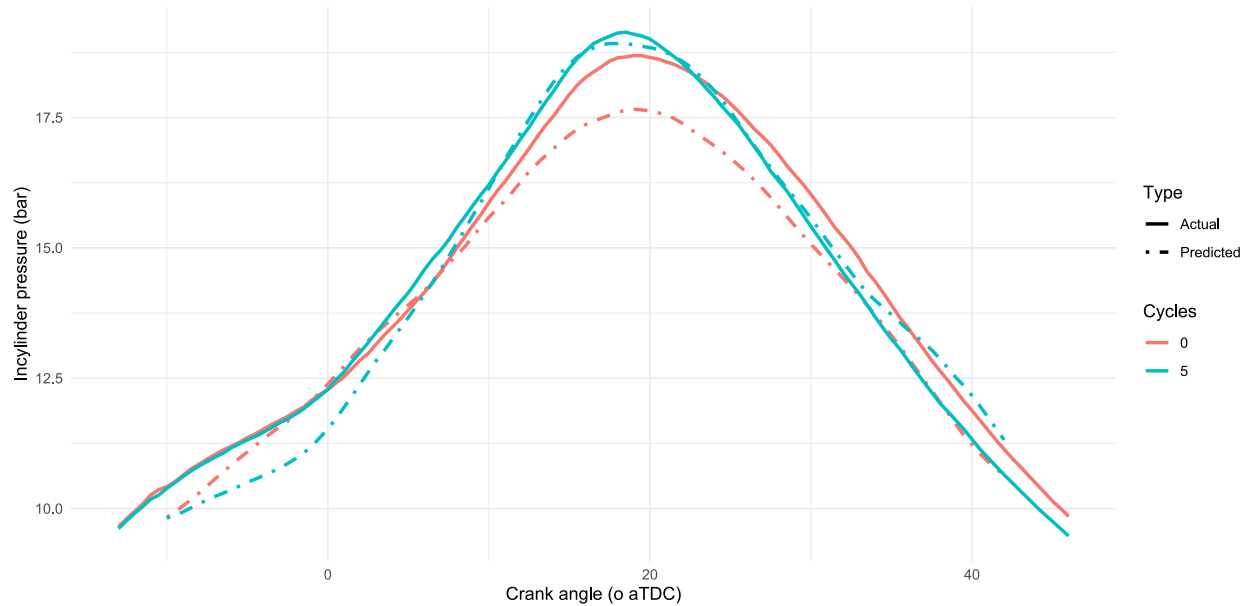
There are different ways to measure CTC differences in how combustion engines work. One option is to use pressure sensors to see how much pressure builds up inside the engine cylinder during each cycle. The sensors take pressure readings cycle by cycle. By analyzing these pressure measurements and calculating the indicated mean effective

pressure (IMEP), it can determine how much the pressure varies from one cycle to the next. This CTC variation in pressure gives insights into how the fuel is burning in the engine.

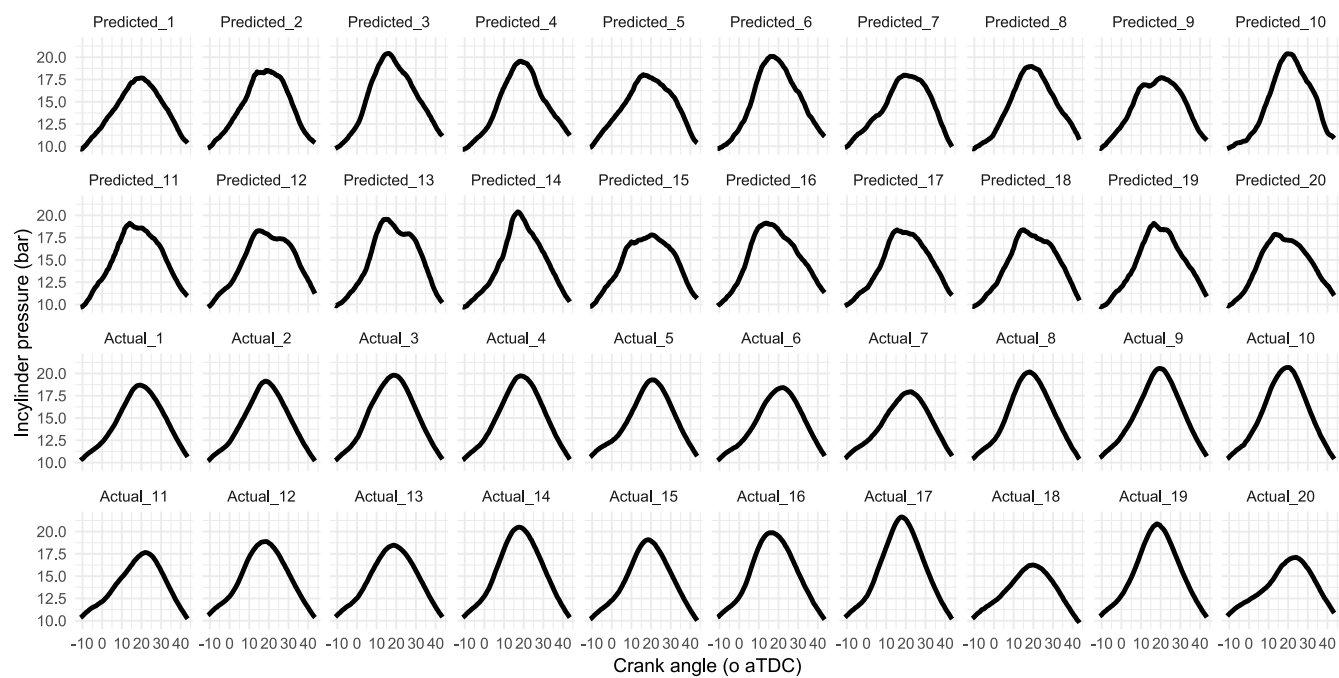
The use of flame images can provide better indications of CTC. In particular, the flame area and propagation were used to calculate COV as an indicator of CTC [45]. The use of cameras in measuring systems has become increasingly popular in recent years due to their ability to provide high-resolution images for in-cylinder processes with more detail. When it comes to combustion analysis, there are several advantages of using a camera to measure CTC variation in combustion engines rather than traditional pressure sensors. Unlike traditional pressure sensors, cameras can capture detailed information about the fuel mixture, ignition timing, and flame propagation, allowing for a more comprehensive understanding of the combustion process. Finally, using ML techniques to analyze images and predict pressure can be more flexible and adaptable. Additionally, such models can be easily updated and refined as new data becomes available, allowing for continuous improvement in engine performance and efficiency.

By utilizing the developed and tested networks in this study, the cycle-to-cycle variation can be predicted using a minimal number of images. Cyclic variations can be quantitatively characterized by parameters related to the cylinder pressure, such as the peak cylinder pressure (P_{max}) or the indicated mean effective pressure (IMEP) [23,46]. Fig. 14 shows the comparison of peak cylinder pressure of measured and predicted cycles using different prediction models. Based on the averaged peak cylinder pressure data for 30 consecutive cycles, EfficientNetB4 and CNN models have the best predicted values compared to the measured data. Followed by Ensemble Adversarial Inception Resnet, CNN-XGBOOST, and finally, ResNet50. The same model ranking is observed when analyzing the engine cyclic variations based on $COV_{P_{max}}$.

Fig. 15 shows the saliency maps for selected cycles. Saliency maps are visualization techniques used to highlight the important regions or features in an input image that contribute most significantly to the prediction made by a model. They provide insights into which parts of the image the model is focusing on to make its decisions by analyzing the gradients of the model's output with respect to the input image pixels to



(a)



(b)

Fig. 13. Actual and predicted pressure values at different crank angles (a) two sample cycles (b) single cycles.

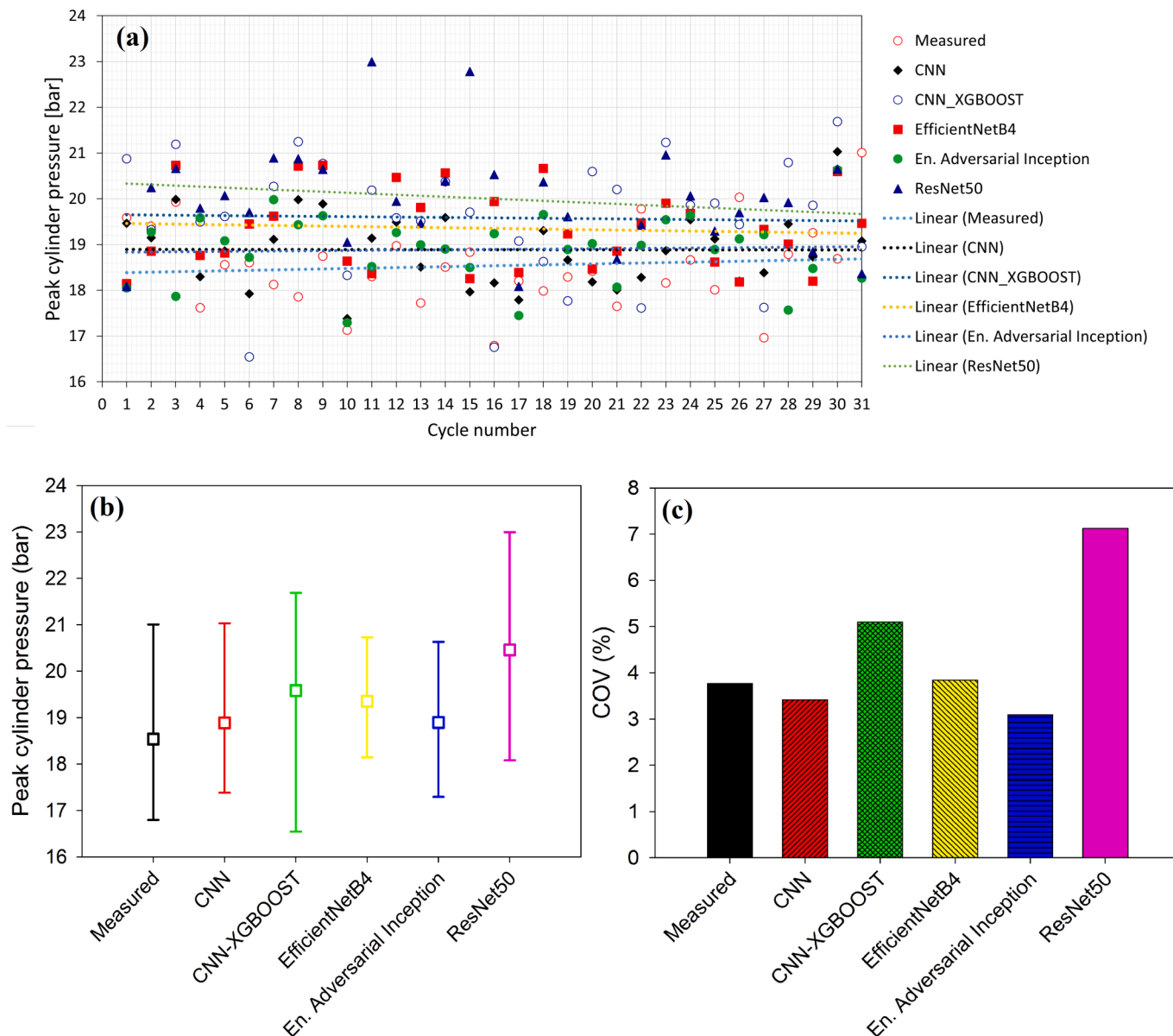


Fig. 14. Comparison of peak cylinder pressure of measured and predicted cycles using different prediction models (a) Cyclic peak cylinder pressure for different cycles (b) Average peak cylinder pressure (c) COV.

determine the importance of each pixel for the final prediction. We used gradient-based saliency mapping to visualize the regions of the input images that contribute most to the model's predictions. The saliency map $\mathcal{M}(I)$ is computed as $\mathcal{M}(I) = \frac{\partial p_l}{\partial I}$ where ∂p_l is the gradient of the model's output p_l (in-cylinder pressure prediction) with respect to the input image ∂I . This gradient shows how changes in each pixel of the input image I affect the predicted output p_l . Higher saliency values indicate more important regions, while lower values correspond to less relevant areas.

In these maps, the higher saliency values are not concentrated in areas with the most intense flame, as one might expect. Instead, the model focuses on regions with more subtle flame characteristics, such as edges or even areas where flames are absent. This suggests that the model is not solely relying on obvious visual cues like flame intensity but is instead detecting smaller, detailed features across the image. The model appears to be using information from the flame's edges and textures, which could provide key information about combustion dynamics.

The scattered distribution of high-saliency areas implies that the

model is using a broad range of features across the entire flame image to make its predictions. This could be beneficial for capturing fine-grained variations in combustion, such as differences in flame propagation or combustion conditions. Furthermore, this distribution reduces the risk of overfitting, as the model is learning to generalize from multiple features rather than focusing on a single prominent area. This indicates a more robust model behavior, making it invariant to small changes in flame orientation, brightness, and positioning, which are likely to occur in real-world applications.

6. Summary and conclusions

This study demonstrates the potential of deep learning models for accurately predicting in-cylinder pressure in combustion engines solely from in-cylinder flame propagation images. The data used for training and testing in this research was obtained by capturing flame images simultaneously with in-cylinder pressure measurement using a test bench of single cylinder optical GDI research engine. By employing state-of-the-art models such as EfficientNetB4, ResNet50, Ensemble

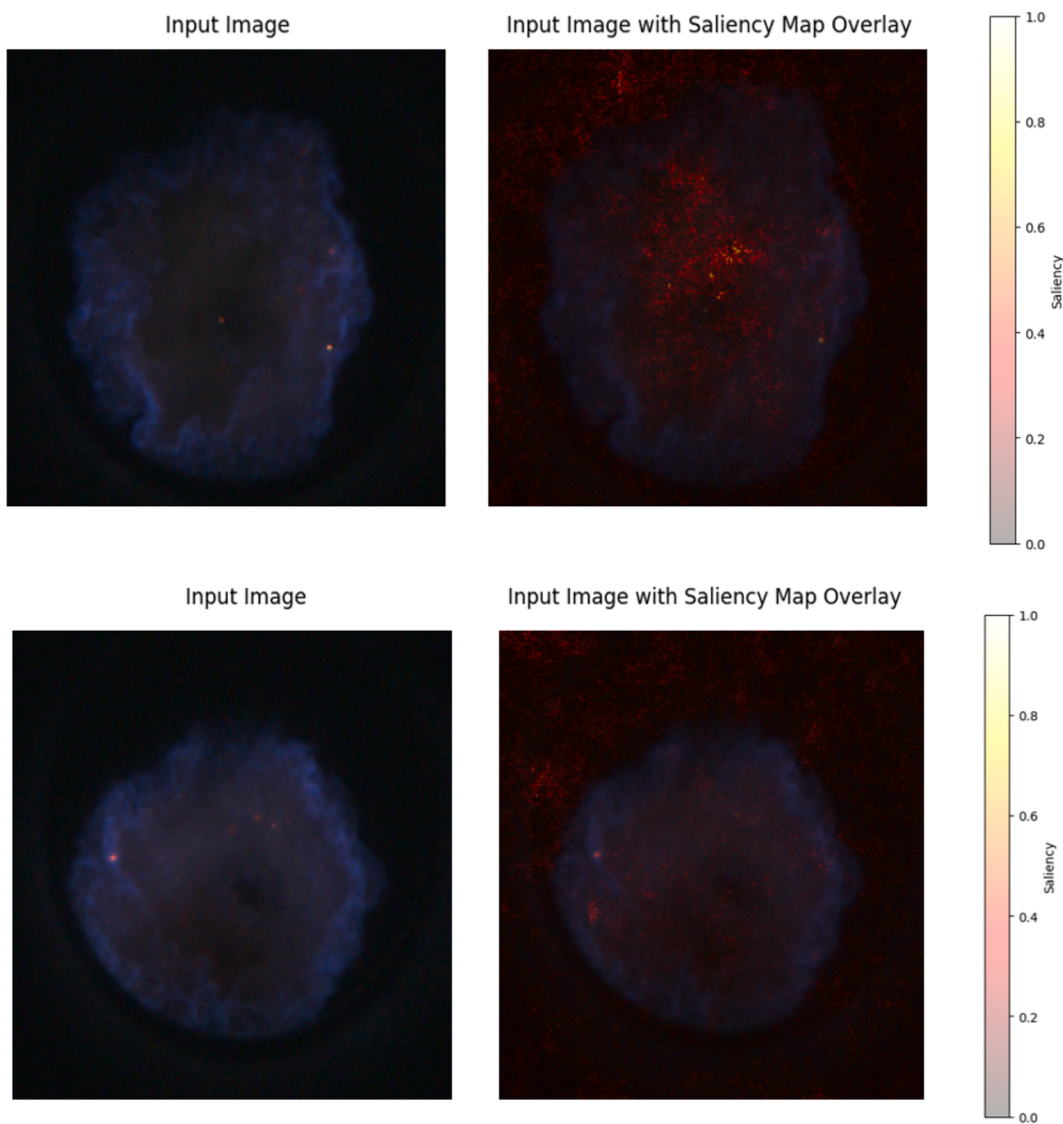


Fig. 15. Saliency maps for different flame images.

Adversarial Inception ResNet, CNN, and CNN-XGBoost, very good results were achieved in terms of predictive performance. The conclusions of this study can be summarized as follows:

- Using a dataset consisting of a total of 1350 images and their corresponding pressure data, each image containing 4000 input pixels/features, multiple deep learning models were trained. These models learned the complex correlations between flame morphology (features) and in-cylinder pressure values. The robustness of the models was evaluated on a separate set of 30 cycles, which included 4500 images. Based on a total of 40 cycles used for the training, validation, and testing, the models exhibited high accuracy and a good capability to predict cycle-to-cycle variations.
- Among the models examined, EfficientNetB4 consistently demonstrated superior performance, exhibiting the highest mean value of R^2 and the lowest RMSE and MAPE when compared to other models. These findings provide further confirmation of its efficacy in capturing cycle-to-cycle variation ($COV_{P_{max}}$) and generating precise predictions for the target variable. As a result, the proposed EfficientNetB4 model holds significant potential for rapid and accurate prediction of in-cylinder pressure data and its variation with time.
- The average predicted pressure data obtained from EfficientNetB4 showed a significant level of agreement with the experimental

measured pressure values, with minimal deviations. The peak pressure values were identical. Nonetheless, the predicted cycles reached their peak pressure slightly earlier than the measured cycles. This occurrence might be attributed to the flame propagating towards the wall, where the trained models anticipated the maximum pressure point earlier than the actual measured peak pressure.

The primary limitation of this study is its focus on a specific operating load and speed for model training and testing. However, this limitation can be addressed through the application of fine-tuning techniques, potentially enabling the model to perform well under various loads and speeds. We propose utilizing transfer learning techniques to ensure the model's adaptability to different engine speeds and loads. This approach is expected to yield satisfactory performance while allowing the models to retain their learned knowledge when applied to datasets representing new operational conditions. A key advantage of this method is its efficiency, requiring minimal additional training data due to the model's existing grasp of primary features.

While implementing high-speed flame imaging in real, multi-cylinder engines, especially in commercial settings, presents challenges, this study serves as a crucial proof of concept. As high-speed imaging technology advances and becomes more cost-effective, the feasibility of adopting these methods in real-time engine applications

will increase. Optical diagnostics offer significant advantages over traditional pressure sensors, providing non-intrusive, high-resolution measurements of in-cylinder processes without disturbing combustion. By integrating this approach with current engine monitoring systems, we can enhance our understanding of combustion dynamics, optimize performance, reduce emissions, and improve long-term engine reliability.

Although this study focuses on pressure prediction, future research should extend this approach to other critical combustion parameters, such as temperature distribution, heat release rate, air-fuel mixture uniformity, and pollutant formation (e.g., NO_x, CO, and unburned hydrocarbons). These factors are essential for a comprehensive understanding of combustion efficiency, engine performance, and emissions. Expanding the model's capabilities to predict these parameters in real-time would lead to more sophisticated engine monitoring systems, potentially improving fuel injection strategies, thermal management, and ultimately resulting in cleaner, more efficient combustion technologies.

CRediT authorship contribution statement

Ahmed Maged: Writing – review & editing, Writing – original draft, Visualization, Software, Methodology, Data curation. **Mohamed Nour:** Writing – review & editing, Writing – original draft, Visualization, Methodology, Data curation, Conceptualization.

Declaration of competing interest

The authors declare that they have no known competing financial interests or personal relationships that could have appeared to influence the work reported in this paper.

Data availability

Data will be made available on request.

Acknowledgment

This research is sponsored by the National Natural Science Foundation of China (NSFC) under grant no. 52150410425.

References

- [1] Huang Q, Liu J, Ulishney C, Dumitrescu CE. On the use of artificial neural networks to model the performance and emissions of a heavy-duty natural gas spark ignition engine. *Int J Engine Res* 2022;23:1879–98. <https://doi.org/10.1177/14680874211034409>.
- [2] Liu Z, Liu J. Machine learning assisted analysis of an ammonia engine performance. *J Energy Resour Technol* 2022;144(11):112307. <https://doi.org/10.1115/1.4054287>.
- [3] Liu J, Huang Q, Ulishney C, Dumitrescu CE. Comparison of random forest and neural network in modeling the performance and emissions of a natural gas spark ignition engine. *J Energy Resour Technol* 2022;144(3):032310. <https://doi.org/10.1115/1.4053301>.
- [4] Liu J, Huang Q, Ulishney C, Dumitrescu C. A support-vector machine model to predict the dynamic performance of a heavy-duty natural gas spark ignition engine. SAE Technical Paper 2021-01-0529 2021. <https://doi.org/10.4271/2021-01-0529>.
- [5] Ihme M, Tong W, Ananda A. Combustion machine learning : Principles, progress and prospects. *Prog Energy Combust Sci* 2022;91:1–57. <https://doi.org/10.1016/j.pecs.2022.101010>.
- [6] Karunamurthy K, Janvekar AA, Palaniappan PL, Adhitya V, Lokeswar TTK, Harish J. Prediction of IC engine performance and emission parameters using machine learning: A review. *J Therm Anal Calorim* 2023;148:3155–77. <https://doi.org/10.1007/s10973-022-11896-2>.
- [7] Zhou L, Song Y, Ji W, Wei H. Machine learning for combustion. *Energy and AI* 2022;7:100128. <https://doi.org/10.1016/j.egyai.2021.100128>.
- [8] Kalogirou SA. Artificial intelligence for the modeling and control of combustion processes: A review. *Prog Energy Combust Sci* 2003;29. [https://doi.org/10.1016/S0360-1285\(03\)00058-3](https://doi.org/10.1016/S0360-1285(03)00058-3).
- [9] Ai B, Wen Z, Wang Z, Wang R, Su D, Li C, et al. Convolutional neural network to retrieve water depth in marine shallow water area from remote sensing images. *IEEE J Sel Top Appl Earth Obs Remote Sens* 2020;13:2888–98. <https://doi.org/10.1109/JSTARS.2020.2993731>.
- [10] Hsu YC, Yu CH, Buehler MJ. Using deep learning to predict fracture patterns in crystalline solids. *Matter* 2020;3:197–211. <https://doi.org/10.1016/j.matt.2020.04.019>.
- [11] Yang Z, Yu CH, Buehler MJ. Deep learning model to predict complex stress and strain fields in hierarchical composites. *Sci Adv* 2021;7. <https://doi.org/10.1126/SCIADV.ABD7416>.
- [12] Fernandez M, Ban F, Woo G, Hsing M, Yamazaki T, Leblanc E, et al. Toxic Colors: The use of deep learning for predicting toxicity of compounds merely from their graphic images. *J Chem Inf Model* 2018;58:1533–43. <https://doi.org/10.1021/acs.jcim.8b00338>.
- [13] Zhao F, Hung DLS. Applications of machine learning to the analysis of engine in-cylinder flow and thermal process: A review and outlook. *Appl Therm Eng* 2023;220:119633. <https://doi.org/10.1016/j.applthermaleng.2022.119633>.
- [14] Wan K, Hartl S, Vervisch L, Domingo P, Barlow RS, Hasse C. Combustion regime identification from machine learning trained by Raman/Rayleigh line measurements. *Combust Flame* 2020;219:268–74. <https://doi.org/10.1016/j.combustflame.2020.05.024>.
- [15] Hwang J, Lee P, Mun S, Karathanassis IK, Koukouvinis P, Pickett LM, et al. Machine-learning enabled prediction of 3D spray under engine combustion network spray G conditions. *Fuel* 2021;293:120444. <https://doi.org/10.1016/j.fuel.2021.120444>.
- [16] Owoyele O, Pal P. A novel machine learning-based optimization algorithm (ActivO) for accelerating simulation-driven engine design. *Appl Energy* 2021;285:116455. <https://doi.org/10.1016/j.apenergy.2021.116455>.
- [17] Ghazaly NM, Moaaz AO, Makrathy MM, Hashim MA, Nasef MH. Prediction of misfire location for SI engine by unsupervised vibration algorithm. *Appl Acoust* 2022;192:108726. <https://doi.org/10.1016/j.apacoust.2022.108726>.
- [18] Sahoo S, Kumar VNSP, Srivastava DK. Quantitative analysis of engine parameters of a variable compression ratio CNG engine using machine learning. *Fuel* 2022;311:122587. <https://doi.org/10.1016/j.fuel.2021.122587>.
- [19] Fu J, Yang R, Li X, Sun X, Li Y, Liu Z, et al. Application of artificial neural network to forecast engine performance and emissions of a spark ignition engine. *Appl Therm Eng* 2022;201:117749. <https://doi.org/10.1016/j.applthermaleng.2021.117749>.
- [20] Cocco Mariani V, Hennings Och S, dos Santos CL, Domingues E. Pressure prediction of a spark ignition single cylinder engine using optimized extreme learning machine models. *Appl Energy* 2019;249:204–21. <https://doi.org/10.1016/j.apenergy.2019.04.126>.
- [21] Liu J, Huang Q, Ulishney C, Dumitrescu CE. Machine learning assisted prediction of exhaust gas temperature of a heavy-duty natural gas spark ignition engine. *Appl Energy* 2021;300:117413. <https://doi.org/10.1016/j.apenergy.2021.117413>.
- [22] Aliramezani M, Koch CR, Shahbakti M. Modeling, diagnostics, optimization, and control of internal combustion engines via modern machine learning techniques: A review and future directions. *Prog Energy Combust Sci* 2022;88:100967. <https://doi.org/10.1016/j.pecs.2021.100967>.
- [23] Hanuschkin A, Zündorf S, Schmidt M, Welch C, Schorr J, Peters S, et al. Investigation of cycle-to-cycle variations in a spark-ignition engine based on a machine learning analysis of the early flame kernel. *Proc Combust Inst* 2021;38:5751–9. <https://doi.org/10.1016/j.proci.2020.05.030>.
- [24] Hanuschkin A, Schober S, Bode J, Schorr J, Böhml B, Krüger C, et al. Machine learning-based analysis of in-cylinder flow fields to predict combustion engine performance. *Int J Engine Res* 2021;22:257–72. <https://doi.org/10.1177/1468087419833269>.
- [25] Kodavasal J, Moiz AA, Ameen M, Som S. Using machine learning to analyze factors determining cycle-to-cycle variation in a spark-ignited gasoline engine. *J Energy Res Technol, Trans ASME* 2018;140. <https://doi.org/10.1115/1.4040062>.
- [26] Di Mauro A, Chen H, Sick V. Neural network prediction of cycle-to-cycle power variability in a spark-ignited internal combustion engine. *Proc Combus Inst* 2019;37:4937–44. <https://doi.org/10.1016/j.proci.2018.08.058>.
- [27] Goodfellow Ian, Yoshua Bengio and AC. Deep learning. MIT Press 2016.
- [28] Ofner AB, Kefalas A, Posch S, Geiger BC. Knock detection in combustion engine time series using a theory-guided 1-D convolutional neural network approach. *IEEE/ASME Trans Mechatron* 2022;27:4101–11. <https://doi.org/10.1109/TMECH.2022.3144832>.
- [29] Yaşar H, Çağıl G, Torkul O, Şıçıcı M. Cylinder pressure prediction of an HCCI engine using deep learning. *Chin J Mech Eng (English Edition)* 2021;34. <https://doi.org/10.1186/s10033-020-00525-4>.
- [30] Gangopadhyay T, De S, Liu Q, Mukhopadhyay A, Sen S, Sarkar S. A deep learning approach to detect lean blowout in combustion systems. *ArXiv Preprint* 2022;1–14. <https://doi.org/10.48550/arXiv.2208.01871v1>.
- [31] Lee S, Lee Y, Lee Y, Shin S, Kim M, Park J, et al. Proposal of a methodology for designing engine operating variables using predicted NO_x emissions based on deep neural networks. *J Mech Sci Technol* 2021;35:1747–56. <https://doi.org/10.1007/s12206-021-0337-2>.
- [32] Shin D, Jo S, Kim HJ, Park S. Application of physical model test-based long short-term memory algorithm as a virtual sensor for nitrogen oxide prediction in diesel engines. *Int J Automot Technol* 2023;24:585–93. <https://doi.org/10.1007/s12239-023-0049-y>.
- [33] Yao S, Wang B, Kronenburg A, Stein OT. Modeling of sub-grid conditional mixing statistics in turbulent sprays using machine learning methods. *Phys Fluids* 2020;32. <https://doi.org/10.1063/5.0027524>.
- [34] Shin S, Kwon M, Kim S, So H. Prediction of equivalence ratio in combustion flame using chemiluminescence emission and deep neural network. *Int J Energy Res* 2023;2023. <https://doi.org/10.1155/2023/3889951>.
- [35] Godwin DJ, Varuvell EG, Martin MLJ. Prediction of combustion, performance, and emission parameters of ethanol powered spark ignition engine using ensemble

- Least Squares boosting machine learning algorithms. *J Clean Prod* 2023;421. <https://doi.org/10.1016/j.jclepro.2023.138401>.
- [36] Ricci F, Petrucci L, Mariani F, Grimaldi CN. Investigation of a hybrid LSTM + 1DCNN approach to predict in-cylinder pressure of internal combustion engines. *Information* 2023;14. <https://doi.org/10.3390/info14090507>.
- [37] Zhuang F, Qi Z, Duan K, Xi D, Zhu Y, Zhu H, et al. A comprehensive survey on transfer learning. *Proc IEEE* 2021;109:43–76. <https://doi.org/10.1109/JPROC.2020.3004555>.
- [38] He K, Zhang X, Ren S, Sun J. Deep residual learning for image recognition. *Proceedings of the IEEE Computer Society Conference on Computer Vision and Pattern Recognition* 2016;2016-Decem:770–8. [Doi: 10.1109/CVPR.2016.90](https://doi.org/10.1109/CVPR.2016.90).
- [39] Nilakshi J, Shwetambari B, Bhavesh P, Vineet K, Mustansir G, Shubham K, et al. Securing Visual Integrity: An Efficient NetB4-Based Solution with Attention Layers and Siamese Training for Face Manipulation Detection in Videos. *IJSAE* 2024;3: 1573–80.
- [40] Tan M, Le Q V. EfficientNet: Rethinking model scaling for convolutional neural networks. *36th International Conference on Machine Learning, ICML 2019* 2019; 2019-June:10691–700.
- [41] Kurakin A, Goodfellow I, Bengio S, Dong Y, Liao F, Liang M, et al. Adversarial attacks and defences competition. *ArXiv Preprint* 2018:195–231. https://doi.org/10.1107/978-3-319-94042-7_11.
- [42] Chen T, Guestrin C. XGBoost: A scalable tree boosting system. *Proceedings of the ACM SIGKDD International Conference on Knowledge Discovery and Data Mining* 2016;13–17-August:785–94. [Doi: 10.1145/2939672.2939785](https://doi.org/10.1145/2939672.2939785).
- [43] Johnson R, Kaczynski D, Zeng W, Warey A, Grover R, Keum S. Prediction of Combustion Phasing Using Deep Convolutional Neural Networks. *SAE Technical Papers*, vol. 2020- April, SAE International; 2020. [Doi: 10.4271/2020-01-0292](https://doi.org/10.4271/2020-01-0292).
- [44] Schiffmann P, Reuss DL, Sick V. Empirical investigation of spark-ignited flame-initiation cycle-to-cycle variability in a homogeneous charge reciprocating engine. *Int J Engine Res* 2018;19:491–508. <https://doi.org/10.1177/1468087417720558>.
- [45] Li J, Zhang R, Pan J, Wei H, Shu G, Chen L. Ammonia and hydrogen blending effects on combustion stabilities in optical SI engines. *Energy Convers Manag* 2023; 280:116827. <https://doi.org/10.1016/j.enconman.2023.116827>.
- [46] Heywood JB, et al. Internal combustion engine fundamentals. New York: McGraw-hill; 1988.